

Journal of Materials Chemistry B

Accepted Manuscript



This is an *Accepted Manuscript*, which has been through the Royal Society of Chemistry peer review process and has been accepted for publication.

Accepted Manuscripts are published online shortly after acceptance, before technical editing, formatting and proof reading. Using this free service, authors can make their results available to the community, in citable form, before we publish the edited article. We will replace this *Accepted Manuscript* with the edited and formatted *Advance Article* as soon as it is available.

You can find more information about *Accepted Manuscripts* in the [Information for Authors](#).

Please note that technical editing may introduce minor changes to the text and/or graphics, which may alter content. The journal's standard [Terms & Conditions](#) and the [Ethical guidelines](#) still apply. In no event shall the Royal Society of Chemistry be held responsible for any errors or omissions in this *Accepted Manuscript* or any consequences arising from the use of any information it contains.

Green silver nanobioarchitectures with amplified antioxidant and antimicrobial properties

Cite this: DOI: 10.1039/x0xx00000x

Received 00th January 2012,
Accepted 00th January 2012

DOI: 10.1039/x0xx00000x

www.rsc.org/

Marcela Elisabeta Barbinta-Patrascu,^a Camelia Ungureanu,^b Stefan Marian Iordache,^c
Ioana-Raluca Bunghez,^d Nicoleta Badea,^b and Ileana Rau*^b,

Cornelian silver-based architectures were achieved from liposomes, silver nanoparticles (AgNPs) and single-walled carbon nanotubes (SWCNTs) by a „green“bottom-up strategy. Liposomes were prepared by thin film hydration method and labelled with a natural porphyrin extracted from spinach leaves – chlorophyll *a* (Chla). Due to its strong visible absorption and fluorescence emission, this phytopigment was used as a spectral sensor to monitor any possible changes occurring in lipid membranes caused by the action of various agents. An aqueous extract from *Cornus mas* L. fruits was used for AgNPs phytosynthesis. Addition of appropriate amounts of phytonanosilver particles and SWCNTs to biomimetic membranes resulted in biohybrid material with good physical stability (ZP = -34 mV), high antioxidant activity (AA = 97.8 %) and has been shown to be strong biocide offering diameters of inhibition zones of 18.3 mm, 23.8 mm and 21.6 mm against *Escherichia coli* ATCC 8738, *Staphylococcus aureus* ATCC 25923 and *Enterococcus faecalis* ATCC 29212, respectively. Chla rapidly sensed the modifications occurred in artificial lipid bilayers as a result of interactions with silver nanoparticles and carbon nanotube surface indicating the biohybrid formation, results supported by AFM analysis. The bioconstructed hybrid material consisting of biomimetic membranes, phyto-nanosilver and SWCNTs could be applied as antimicrobial and antioxidant coating.

INTRODUCTION

Nanotechnology, one of the youngest and most exciting multidisciplinary research fields has known great progress in recent years.

Since their discovery by Sumio Iijima in 1991¹ carbon nanotubes (CNTs) gained more and more interest in nanotechnological research area. Carbon nanotubes are carbon allotropes constructed of cylindrical graphene sheets that are planar honeycomb lattice structures of *sp*² hybridized carbon atoms. These *sp*² in-plane bonds are the strongest bonds in nature and confer unusual properties to CNTs that exceed those of any existing materials^{2,3}.

Carbon nanotubes are used as building blocks to design novel nanomaterials with improved properties⁴. Recently, carbon nanotube-based drug delivery systems have attracted significant attention in nanomedicine to fight against cancer⁵⁻⁷.

^aUniversity of Bucharest, Faculty of Physics, Department of Electricity and Magnetism, Solid-State Physics, and Biophysics, 405 Atomistilor Street, PO Box MG-11, Bucharest-Magurele, 077125, Romania

^bPOLITEHNICA University of Bucharest, Faculty of Applied Chemistry and Materials Science 1-7, Polizu Str., 011061, Bucharest, Romania

^cUniversity of Bucharest, Faculty of Physics, 3Nano-SAE Research Centre, PO Box MG-38, Bucharest-Magurele, 077125, Romania

^dNational Institute for Research & Development in Chemistry and Petrochemistry INCDCP-ICECHIM, 202 Spl. Independentei, Bucharest, 060021, Romania

In the last decade, the nanotechnological research focused on nanostructures allowed the development of novel strategies to design exciting materials with very interesting features. Last years, nano-scaled particles have been more and more attracted the attention of the scientists. Nanoparticles offer unique properties that are not available in the bulk materials.^{8,9}

Silver nanoparticles (AgNPs) are the most widely used nano-sized particles in various fields of nanotechnology, especially in biomedical applications as drug delivery systems¹⁰⁻¹² or in cancer therapy¹³. Nanocomposites based on nano-silver exhibit enhanced antibacterial properties^{14,15}. Recently, the superior microbiostatic effects of AgNPs were exploited to construct novel silver-based nanocomposites¹⁶ and silver nanoparticle-filled nylon 6 nanofibers¹⁷ with improved antibacterial properties.

The principles of „green” chemistry in AgNPs synthesis gained a great interest in order to reduce the substances harmful to humans and environment. Natural raw materials are needed to replace the synthetic ones to avoid toxicity or side effects. Plants have a huge bioreducing potential and have been exploited to phytosynthesize nano-scaled silver particles¹⁸⁻²².

Other building blocks for nanotechnology are *phospholipids* – the main components of biomembranes that have become in the last period very attractive soft materials that can be used in various applications^{18, 23-25}. Aryal *et al.* obtained lipid-polymer hybrid nanoparticles with enhanced cytotoxicity against human ovarian cancer cells²⁶. A new and efficient sensor for Fe(III) detection, having an active lipid monolayer have been developed by Duc and co-workers²⁷. Recent scientific papers reported the use of lipids and liposomes for noncovalent functionalization of carbon nanotubes leading to interesting materials^{23, 28-30}.

Liposomes are lipid vesicles made of one or more lipid bilayers (*lamellae*) separated by aqueous compartments. Since the structure of their artificial lipid bilayers mimic that of natural membranes, liposomes, named for this reason „biomimetic membranes”, are widely used in medical and pharmacological applications as drug delivery systems or as model membranes^{23,31}.

In this study, silver nanoparticles, biomimetic membranes (liposomes) and carbon nanotubes were used to originally build up 3-D architectures with improved properties, via a *green bottom-up* approach.

Silver nanoparticles (AgNPs) phyto-synthesized from a natural source (fruits of *Cornus mas* L.) are used as „green” building blocks to design new materials with interesting properties. Cornelian cherries are known to possess antioxidant³²⁻³⁴ and antibacterial^{35,36} properties due to their content of bioactive molecules.

Chlorophyll *a* (Chla) was incorporated in liposomal membranes from three main reasons: 1) Chla molecules exhibit strong absorption and fluorescence emission in the visible (VIS) region of light spectrum and then it was embedded in liposomes as a spectral marker or molecular sensor to monitor the interactions occurring in the biomimetic membranes. Our previously studies reported that Chla is a suitable sensor to detect any modification happened in the artificial lipid bilayers, at molecular level³⁷⁻⁴². 2) Chla is a natural pigment occurred in plants, so many natural resources are abundantly found in nature; in this work spinach leaves were used to isolate this phyto compound.

3) Chla is recognized to possess antioxidant⁴³⁻⁴⁵ and antimicrobial⁴⁶⁻⁴⁸ properties.

The method presented in this paper is simple and low cost, small quantities are needed to achieve improved antioxidant and antimicrobial activities. Some components of the obtained bioconstructs (the phyto compounds coming from cornelian extract and the phospholipids) offer biocompatibility if used in biomedical applications. Natural resources such as plant extracts are safe, widely available and cost-effective.

Different biophysical methods were used to characterize the obtained biohybrids: absorption and fluorescence emission spectroscopy, Dynamic Light Scattering measurements, Atomic Force Microscopy analysis, chemiluminescence technique, antimicrobial assay.

The properties of resulting biohybrid materials (good stability, antioxidant and antimicrobial activities) could be exploited in biotechnological or biomedical applications.

MATERIALS AND METHODS

Materials

Silver nitrate, KH₂PO₄, Na₂HPO₄, luminol (5-amino-2,3-dihydrophthalazine-1,4-dione), Tris (hydroxymethylaminomethane base), HCl, H₂O₂ were purchased from Merck (Germany). Dipalmitoyl phosphatidylcholine (DMPC), chloroform and single-walled carbon nanotubes (SWCNTs) were supplied from Sigma Aldrich (Germany).

The antibacterial activity was tested against three microbial strains such as *Escherichia coli* ATCC 8738, *Staphylococcus aureus* ATCC 25923 and *Enterococcus faecalis* ATCC 29212. The bacterial strains were grown in Luria Bertani Agar (LBA) plates at 37 °C with following composition: peptone (Merck), 10 g/L; yeast extract (Biolife) 5 g/L, NaCl (Sigma-Aldrich) 5 g/L and agar (Fluka) 20 g/L. The stock culture was maintained at 4 °C.

Phytosynthesis of silver nanoparticles

An aqueous *Cornus mas* L. extract of light red colour was obtained from dried fruits using a procedure previously described¹⁸ and further used to prepare silver nanoparticles. This extract played dual role of reducing silver ions (coming from the 1mM AgNO₃ solution) and of stabilizing the silver nanoparticles. Visually, the phytofabrication of AgNPs was evidenced by the colour changing of cornelian cherry extract after addition of AgNO₃, from light red to dark reddish brown caused by the excitation of surface plasmon vibrations in the silver nanoparticles. A mirror like illumination on the flask walls appeared. These two observations confirmed the synthesis of nanosilver. The green approach followed to obtain these AgNPs was previously reported¹⁸.

Preparation of liposomes

Thin film hydration method⁴⁹ was used to prepare DMPC multilamellar lipid vesicles (MLVs, 0.5 mM) labelled with chlorophyll *a* (Chla/lipid molar ratio = 1/100). DMPC lipid membranes were obtained in a liquid crystalline state and under physiological conditions by using already published procedure^{37,38}; the multilamellar vesicles were suspended in a phosphate buffer

solution (PB, KH_2PO_4 - Na_2HPO_4 pH 7.4). Chla was extracted from fresh spinach (*Spinacia oleracea* L.) leaves according to Strain & Svec procedure⁵⁰.

Preparation of biohybrids

Specific aliquot of resuspended SWCNTs in PB pH 7.4 was mixed with an appropriate volume of MLVs suspension into a final ratio of 0.05 mg/mL and with *Cornus mas*-AgNPs (AgNPs:MLVs= 1:30, v/v). This mixture was subjected to an ultrasound treatment (Hielscher titanium probe sonicator, UP 100 H) resulting in liposomes/cornelian-AgNPs/SWCNTs hybrids. The silver presence in AgNPs and biohybrid was confirmed by X-ray fluorescence technique, as previously reported¹⁸.

All experiments were conducted in dark to avoid photodamage of the samples. Figure 1 imaged a schematic representation of „green“ synthesis of silver nanoparticles and of biohybrids (based on liposomes, *Cornus mas*-nanosilver and carbon nanotubes) using an aqueous cornelian cherry extract. The sample codes are presented in Table 1.

Table 1 The sample codes

Sample	Code
<i>Cornus mas</i> L. fruits extract	A
<i>Cornus mas</i> -AgNPs	B
Chla-DMPC-MLVs	C
<i>Cornus mas</i> -AgNPs/Chla-DMPC-MLVs/CNTs hybrids	D

carbon nanotubes) preparation using an aqueous cornelian cherry extract

General analysis

The absorption spectra were acquired in the 300-800 nm range on a double beam UV-VIS spectrophotometer Lambda 2S Perkin Elmer operated at a resolution of 1 nm.

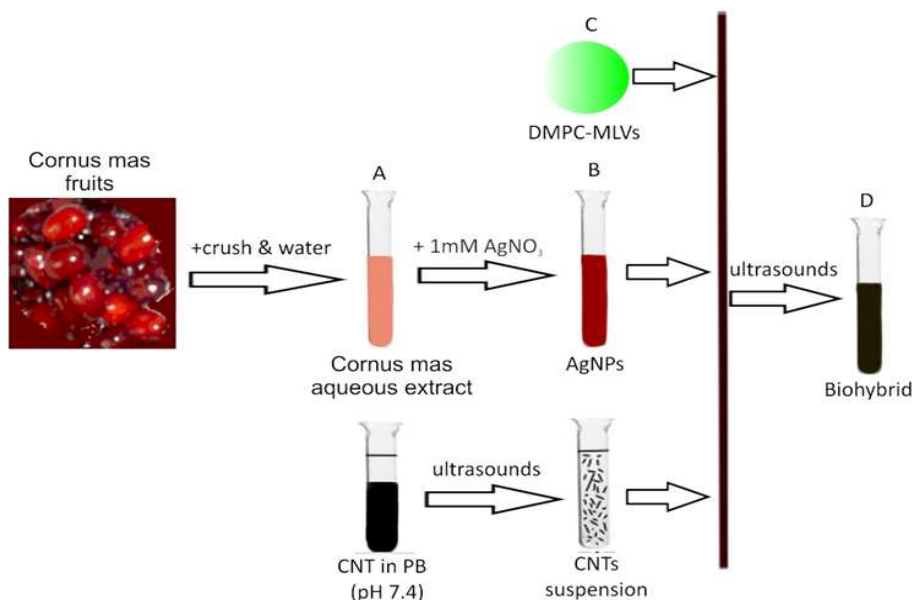
The fluorescence emission spectra of Chla in liposomes and biohybrids were recorded on a Perkin Elmer LS 55 fluorescence spectrometer by sample illuminating with a 430 nm excitation light. The fluorescence emission data were collected in the wavelength range of 600–800 nm.

The Atomic Force Microscopy (AFM) images of silver-based materials were recorded on Integrated Platform SPM-NTegra model Prima in tapping mode using a NSG01 cantilever with a typical curvature radius of 10 nm.

The size of particles given by the hydrodynamic diameters, Zaverage (the particle diameter plus the double layer thickness) was determined using Dynamic Light Scattering technique (Zetasizer Nano ZS, Malvern Instruments Ltd., U.K.), in the range between 0.6 nm and 6.0 μm , at 25 °C temperature and at a scattering angle of 90°. The mean diameters (calculated based on Stokes-Einstein equation) and the polydispersity indexes (PdI, the width of the size distribution) were measured using intensity distribution from 3 individual experiments.

The measurement of electrokinetic potential is used to assess the charge stability of a disperse system. Zeta potential (ZP) measurements were performed in triplicate, by using the appropriate dispositive of Zetasizer Nano ZS (Malvern Instruments Ltd., U.K.) by applying an electric field across the analyzed aqueous dispersion.

Fig. 1 Schematic representation of silver nanoparticles and biohybrid (based on liposomes, *Cornus mas*-nanosilver and



Chemiluminescence (CL) assay

The *in vitro* antioxidant behavior of the samples has been evaluated by chemiluminescence (CL) assay using a Chemiluminometer Turner Design TD 20/20, USA. The oxidative degradation of luminol (a cyclic hydrazide used as light amplifying substance) occurred in the presence of hydrogen peroxide (H_2O_2) in TRIS-HCl buffer solution (pH = 8.6) resulted in a wide range of free radicals of oxygen. The analysis CL system contains: 700 μL TRIS-HCl buffer solution (pH 8.6), 200 μL luminol (10^{-5} M), 50 μL sample and 50 μL of hydrogen peroxide (10^{-5} M). The standard represents the reaction mixture without the sample and is composed of: 750 μL TRIS-HCl buffer solution (pH 8.6), 200 μL luminol (10^{-5} M) and 50 μL hydrogen peroxide (10^{-5} M). Each time, the hydrogen peroxide has been introduced the last. The percentage of free radical scavenging was quantified by calculating the antioxidant activity (AA %) of each sample using the relation:

$$\text{AA} = [(I_0 - I) / I_0] \cdot 100\% \quad (1)$$

where I_0 is the maximum CL intensity for standard (i.e. the reaction mixture without the sample) at $t = 5$ s and I is the maximum CL intensity for sample at $t = 5$ s.²⁴

Antibacterial assay

The agar-well diffusion method was used to evaluate the antibacterial activity of all the samples against some human pathogenic microbial strains: *Staphylococcus aureus* ATCC 25923, *Enterococcus faecalis* ATCC 29212 and *Escherichia coli* ATCC 8738. Sterile Luria Bertani Agar plates were prepared by pouring the sterilized media in sterile Petri dishes under aseptic conditions. The test microorganism 1 mL was spread on agar plates. Wells of 6 mm in diameter were punched into the inoculated agar media with sterile Durham tube. A volume of 50 μL of each sample was dropped into each well. All the plates containing bacteria were incubated at 37 °C for 24 h. Distilled water served as a negative control. The antibacterial activity was interpreted from the size of inhibition zone diameter which was measured in mm from observation of clear zones surrounding the wells. Each sample was assayed in triplicate in order to calculate the mean value (presented as mean \pm standard deviation, SD). Standard deviation was calculated as the square root of variance using STDEV function in Excel 2010.

RESULTS AND DISCUSSION

Characterization of the samples by UV-VIS absorption spectroscopy

The phytosynthesis of silver nanoparticles using the aqueous extract of *Cornus mas* L. fruits (see section *Phytosynthesis of silver nanoparticles*) was evaluated by UV-VIS absorption spectroscopy. Figure 2A presents comparatively the absorption spectra of cornelian aqueous extract (sample A) and *Cornus mas*-AgNPs (sample B). In

the spectral window between 400–500 nm, the *Cornus mas* extract alone showed no maximum, but when exposing to 1 mM AgNO_3 solution, a single peak at 450 nm appeared characteristic for silver nanoparticle formation.⁵¹⁻⁵⁴ This absorption maximum corresponds to the *surface plasmon resonance* (SPR) of conducting electrons from the surface of AgNPs, the presence of SPR band being a signature of the biosynthesis of spherical-shaped silver phytonanoparticles.^{22,55} The *Cornus mas* extract proved to have strong reducing power for phytosynthesis of silver nanoparticles.

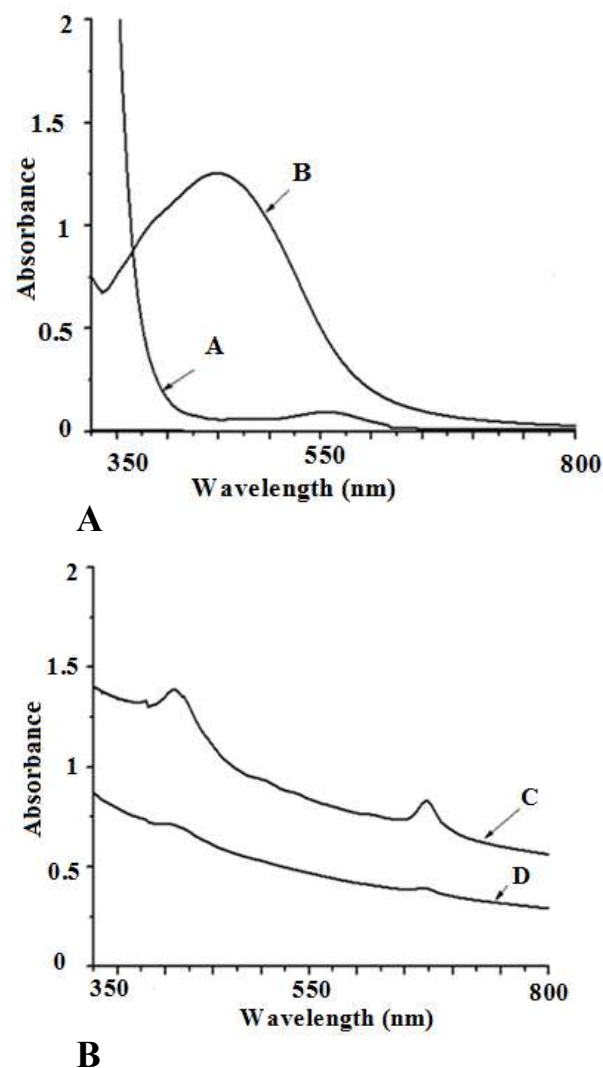


Fig. 2 The absorption spectra of A) cornelian aqueous extract (sample A) and *Cornus mas*-AgNPs (sample B) and of B) Chla-containing samples: Chla-DMPC-MLVs (sample C) and biohybrids (sample D).

Chla embedded in biomimetic membranes was used as a spectral marker to monitor the changes occurred in the artificial lipid bilayers at molecular level. The Chla red absorption maximum in Chla-labeled liposomes is slightly blue-shifted from 672 nm to 669 nm (Figure 2B) after exposure to ultrasounds in presence of AgNPs and SWCNTs, so the location of this phytopigment in the artificial lipid

membranes was modified. These spectral changes in the absorption spectrum of Chla embedded in liposomes indicate a new arrangement of the pigment molecules in the artificial lipid bilayers probably caused by the closeness of the surface of carbon nanotubes, the nanosilver facilitating this modification of Chla position.

The spectral features of Chla can provide a rapid estimation of the size of lipid vesicles.^{37,38} The spectrum of biohybrids (sample D) presented a lower baseline position as compared to that of MLVs (sample C) spectrum, so we could predict that MLVs have bigger size than hybrid material.

Characterization of silver-based biohybrids by fluorescence emission spectroscopy

Figure 3 displays the fluorescence emission spectra of the liposomes and hybrids. Chla incorporated in biomimetic membranes was used as a fluorescent probe.

The fluorophore is represented by the porphyrin macrocycle of Chla. The chlorophyll molecule is placed in the artificial lipid bilayer with the macrocycle at the interface with the aqueous phase in the proximity of polar heads of lipids, and with the phytol tail in the hydrophobic fatty acyl chains region,⁵⁶ providing a better understanding of what it is happening both in the hydrophobic and in the hydrophilic regions of liposomal membranes.

The fluorescence signature of Chla, a natural dye, was significantly quenched by SWCNT presence; this quenching agrees with our previously studies.²⁸ Recent scientific papers reported the use of SWCNTs as an effective quencher for various dyes^{5,6} decreasing their fluorescence intensities through electronic mechanisms.

The dramatic decrease of Chla fluorescence signal after addition of SWCNTs and *Cornus mas*-AgNPs to the suspensions of lipid vesicles could be the result of a more efficient energy transfer between the chlorophyll molecules (embedded in liposomes) interacting with the carbon nanotubes.

As a result of interaction with SWCNTs and AgNPs, a slightly blue shift from 681 nm to 679 nm of the peak emission of Chla it was observed which could be explained by a less polar environment sensed by the fluorophore due to the closeness of the CNT surface.

Both the quenching of Chla fluorescence signal and the blue shift of the peak emission of Chla confirmed the formation of biohybrids based on biomimetic membranes, AgNPs and SWCNTs (Figure 3, sample D).

Evaluation of physical stability of the nanomaterials

The physical stability of the samples was evaluated in terms of zeta potential (ZP) which reflects the electric charge on the particle surface by measuring the electrophoretic mobility of the samples in an electric field. Figure 4 presents comparatively the zeta potential

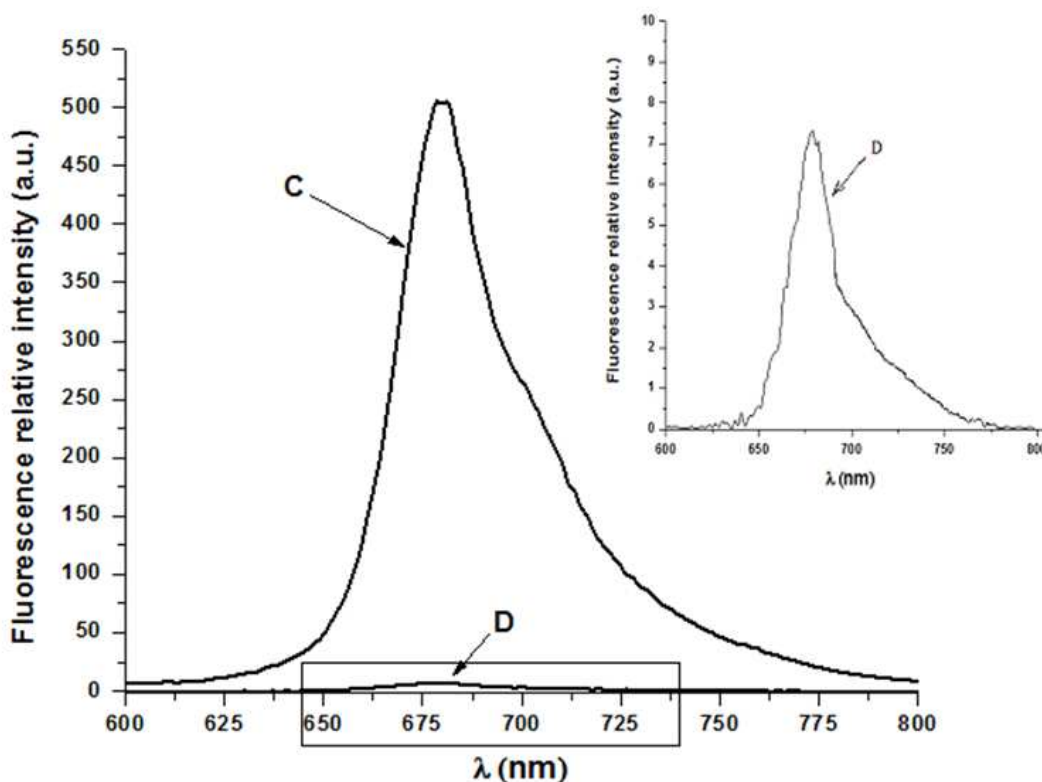


Fig. 3 Fluorescence emission spectra of Chla in liposomes (sample C) and *Cornus mas*-AgNPs-DMPC-CNTs hybrids (see inset, sample D); the excitation wavelength was 430 nm.

Inset: enlarged image of emission spectrum of sample D.

distribution of liposomes and of silver-based nanomaterials.

All the samples displayed negative surface charge providing repulsive forces necessary for the dispersion stability. So, higher negative ZP values lead to more tendency of repulsion between particles and thus preventing particle aggregation.⁵⁷ The suspension

of multilamellar lipid vesicles are low stable ($ZP = -18.4$ mV) as compared with the green silver nanoparticles which presented a moderate stability possessing a mean zeta potential value of -25.9 mV.

The biohybrids exhibited highest physical stability ($ZP = -34$ mV), their suspensions being stable through interparticle electrostatic repulsions. The addition of carbon nanotubes in these hybrid systems enhanced the stability of the biohybrids, results which are consistent with our previous research work.²⁸

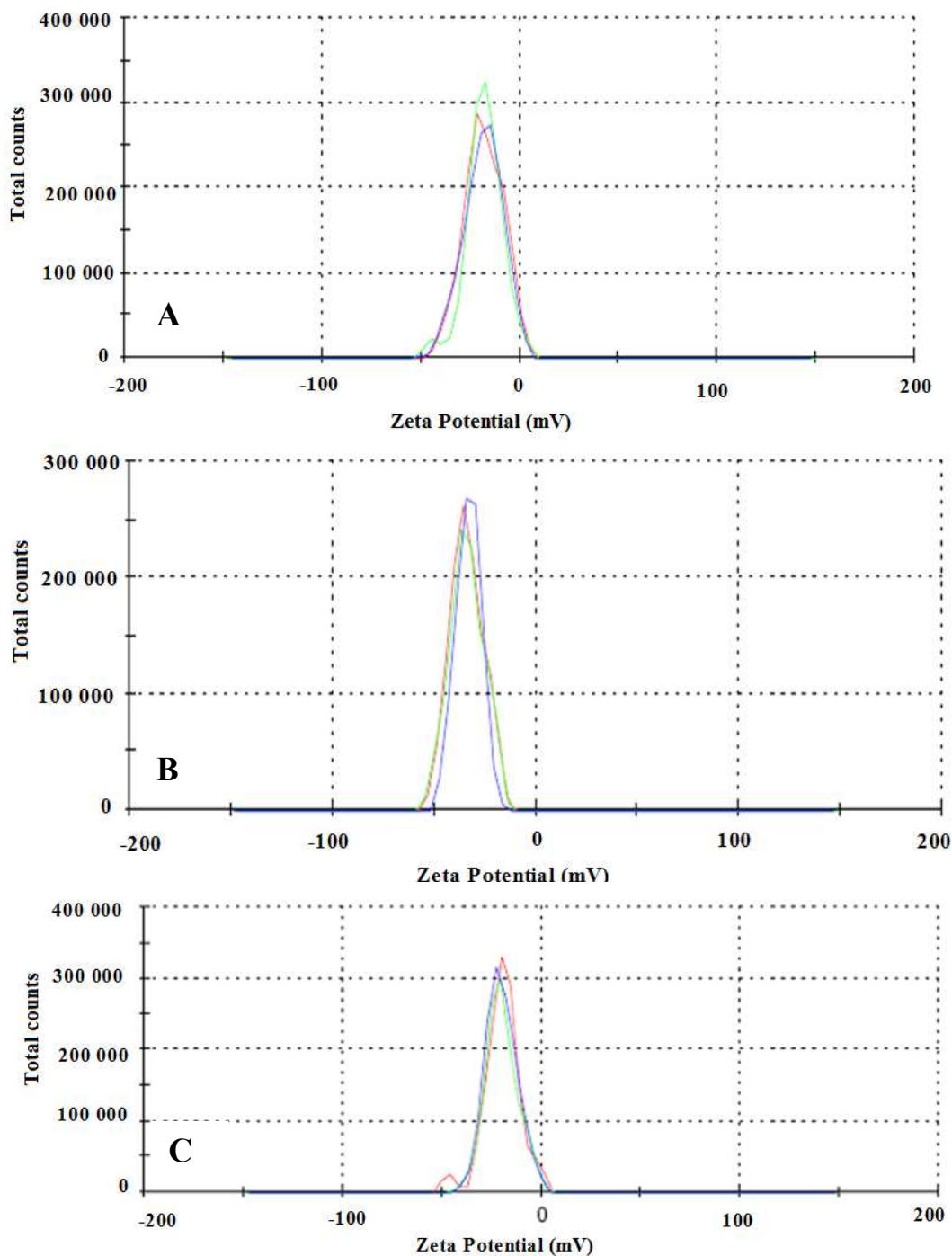


Fig. 4 Comparison of zeta potential distribution of A) *Cornus mas*-AgNPs, B) Chla-DMPC vesicles and C) *Cornus mas*-AgNPs-DMPC-SWCNTs biohybrid

Size determination and morphological characterization of cornelian silver-based architectures

Dynamic Light Scattering (DLS) technique was used to evaluate the dimension of the samples. The hydrodynamic diameters (based on Stokes-Einstein equation) and the polydispersity index (PDI) were achieved from 3 individual measurements using intensity distribution. The results are reported as mean value \pm standard deviation.

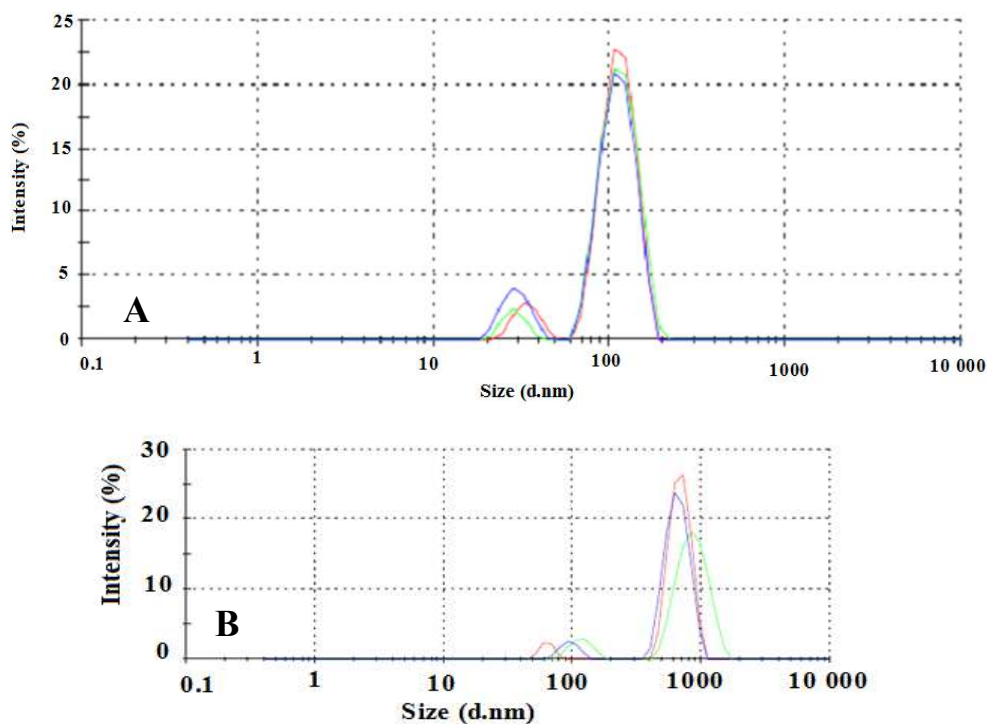
DLS measurements revealed a bimodal particle size distribution profile of the samples (Figure 5). Multilamellar liposomes exhibited an average diameter of 842.5 nm with a high value of polydispersity index (PDI = 0.607) indicating a large distribution of particle size with multiple population of lipid vesicles, being in accordance with the protocol of preparation (see section Preparation of liposomes), confirming the formation of MLVs.

The silver phytonanoparticles presented a hydrodynamic average diameter of 118.7 nm and a good value of polydispersity index (PDI = 0.220) illustrating the presence of quite homogenous population of particles.

The mean diameter of biohybrids based on „green“ nano-silver, carbon nanotubes and biomimetic membranes was found to be 264.8 nm and PDI = 0.332. These biohybrids are smaller in size than MLVs, results that were predicted by absorption spectroscopy (see paragraph Characterization of the samples by UV-VIS absorption spectroscopy).

The morphological aspects of the samples were provided by Atomic Force Microscopy (AFM). Phytosynthesis of nano-scaled silver particles was clearly observed by AFM analysis (Figure 6). Three dimensional (3-D) investigations revealed spherical and quasispherical shaped silver nanoparticles with size ranging between 30 and 210 nm and a slight tendency to aggregate. These findings are in agreement with the DLS and zeta potential measurements. The morphology of the „green“ silver nanoparticles is good correlated to their absorption spectra which exhibited only one SPR band.

The surface topography of the silver phytonanohybrids was imaged in Figure 7. AFM investigation of *Cornus mas*-AgNPs-DMPC-CNTs hybrids revealed the formation of tubular structures consisting in de-agglomerated carbon nanotubes coated with nanosilver-embedded lipid layers. The chlorophyll-containing DMPC lipid membranes are in a liquid crystalline state facilitating the penetration of AgNPs into them during the sonication process. The ultrasound irradiation resulted in de-agglomeration of carbon nanotubes which were decorated with biomimetic membranes and phytonanosilver. The DMPC phospholipids facilitate the de-bundling of CNTs via hydrophobic and *van der Waals* interactions between the fatty acyl chains of DMPC and SWCNT sidewall.



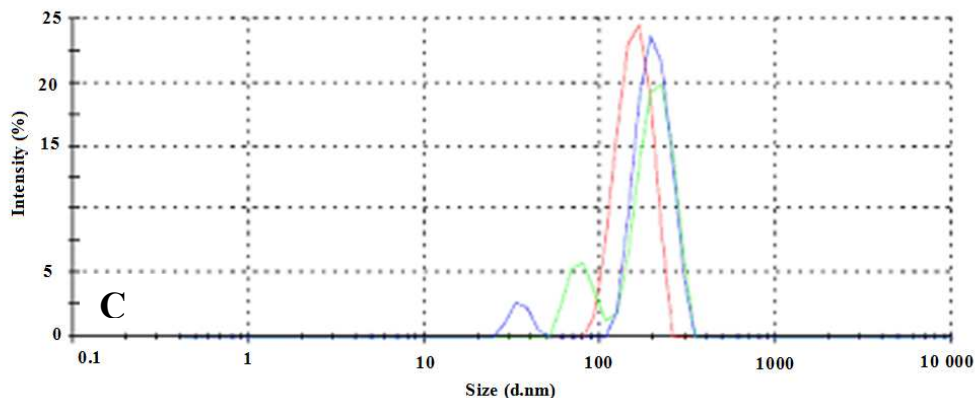


Fig. 5 Particle size distribution of A) *Cornus mas*-AgNPs, B) Chla-DMPC-MLVs and C) *Cornus mas*-AgNPs/Chla-DMPC-MLVs/CNTs biohybrid (sample D).

The soft biological material (DMPC membranes) together with the „green“ silver nanoparticles were supramolecular self-assembled along the carbon nanotubes by ultrasound treatment. The porphyrin ring of chlorophyll located in the liposomes at the lipid-water interface in the vicinity of polar lipid heads allows the binding of Chla molecules via π - π stacking on CNT polyaromatic graphene surface, being able to intermediate the functionalization of carbon nanotubes, findings revealed by a strong quenching of Chla fluorescence signal (see Characterization of silver-based biohybrids by fluorescence emission spectroscopy).

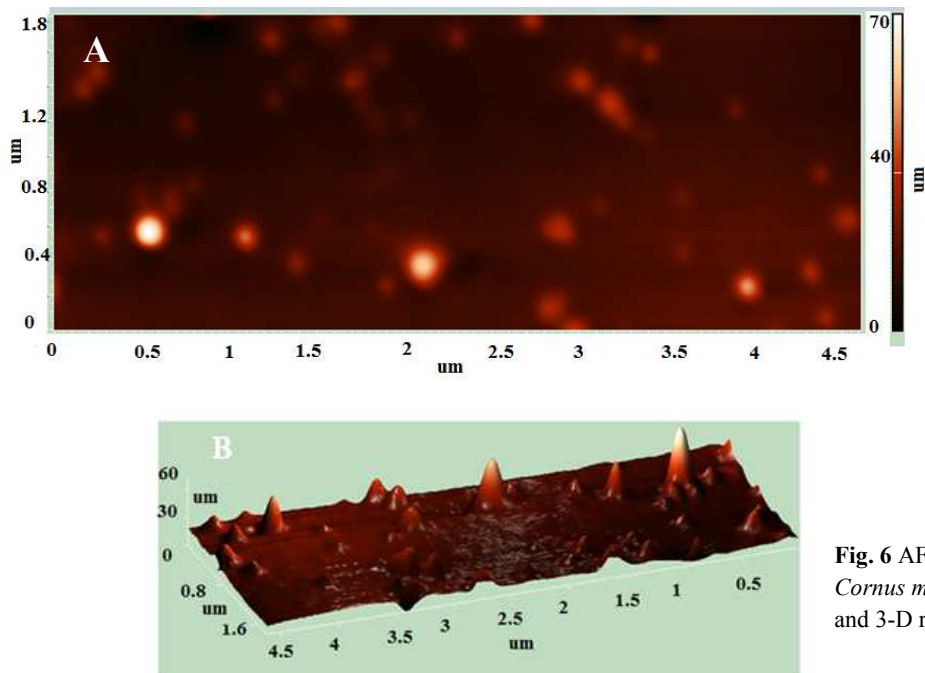


Fig. 6 AFM micrographs of *Cornus mas*-AgNPs in height (A) and 3-D representation (B).

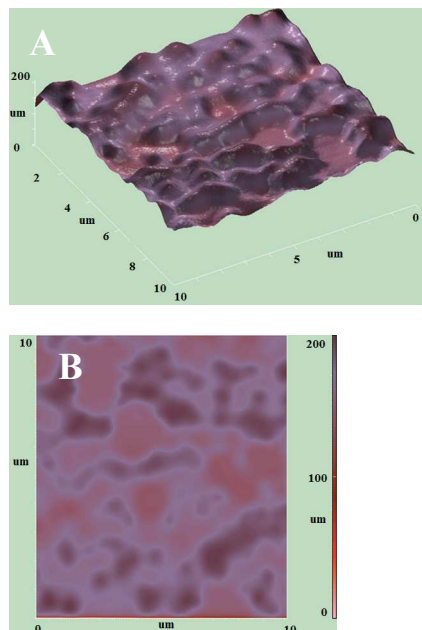


Fig. 7 AFM micrograph of *Cornus mas*-AgNPs-DMPC-CNTs biohybrids in A) 3-D representation and B) height profile.

Antioxidant properties of biohybrids

Chemiluminescence assay was used to evaluate the antioxidant potential of the samples. Quenching of the chemiluminescence signal is direct related with the capacity of the samples to scavenge the free radicals. In order to assess their antioxidant activities, the samples were exposed to a free radical generator system consisting of H_2O_2 in alkaline TRIS-HCl (pH = 8.6) buffer solution that gives rise to a large variety of free radicals with high energy that mimic an oxidative stress *in vitro*. The oxidative degradation of luminol (LH_2) in presence of hydrogen peroxide in alkaline aqueous solutions resulted in a wide range of free radicals such as: hydroxyl radicals (HO^\bullet), superoxide radicals ($O_2^{\bullet-}$), diazasemiquinone radicals (L^\bullet).⁵⁸⁻⁶⁰

The chemiluminescence kinetic profiles of the samples (Fig. 8) revealed a strong decay of CL signals in the case of *Cornus mas* L. fruits extract, *Cornus mas*-AgNPs and the *Cornus mas*-AgNPs/Chla-DMPC-MLVs/CNTs hybrids due to their powerful free radical scavenging capacity, the most potent being the biohybrids. The figure inset presents CL signals in the presence and absence of hybrid materials.

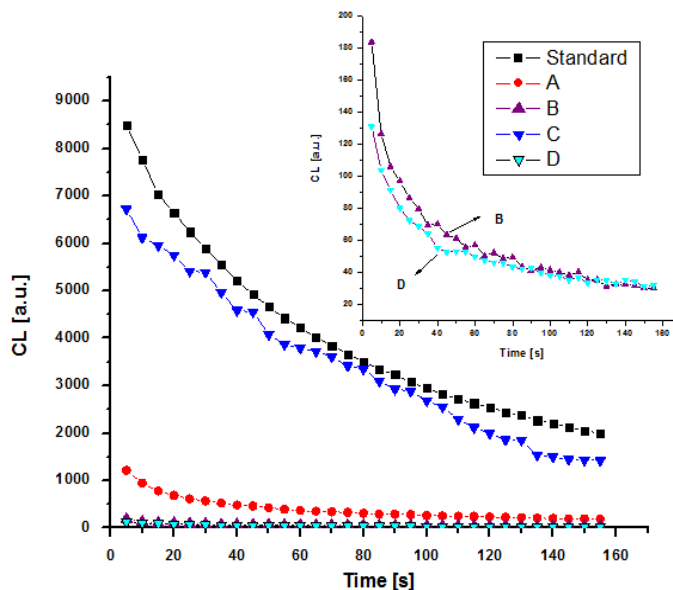


Fig. 8. The chemiluminescence kinetic profiles of CL signals of the samples: A \square *Cornus mas* L. fruits extract, B \square *Cornus mas*-AgNPs, C \square Chla-DMPC-MLVs, D \square *Cornus mas*-AgNPs/Chla-DMPC-MLVs/CNTs hybrids as compared to standard system (the reaction mixture without samples).

The antioxidant profiles displayed in Figure 9 revealed that all the samples possess antioxidant properties.

The beneficial effect of cornelian cherry fruits on human health it is widely recognized for a long time due to their phyto-chemical composition rich in antioxidants, thus, the aqueous *Cornus mas* extract exhibited a notable free radical scavenging capacity (AA = 85.7 %). Our previous studies showed that the addition of 1 mM $AgNO_3$ aqueous solution to the plant extracts resulted in formation of AgNPs with better antioxidant properties.^{18,20} So, the phytosynthesized nano-scaled silver particles (*Cornus mas*-AgNPs) exhibited strong antioxidant properties (AA = 91.4 %).

Chlorophyll *a*, a natural antioxidant, embedded into artificial lipid bilayers (Chla/lipid molar ratio = 1/100) confers antioxidant behavior (AA = 20.9 %) to liposomes.

Small amounts of cornelian silver nanoparticles (AgNPs/MLVs = 1/30, v/v) and carbon nanotubes (0.05 mg/mL) added to Chla-DMPC-MLVs strongly amplified the antioxidant properties of the liposomes. This increase in antioxidant activity is caused by a complex of factors including the plant extract and also the nanometer nature of AgNPs and CNTs. On the other hand, carbon nanotubes possess antioxidant activity due to their continuum π - π conjugated structure derived from sp^2 -hybridized carbon hexagonal nanostructure of CNTs.⁶¹ The percentage of free radical scavenging of the resulted biohybrids (*Cornus mas*-AgNPs/Chla-DMPC-MLVs/CNTs) reached the value of 97.8 %.

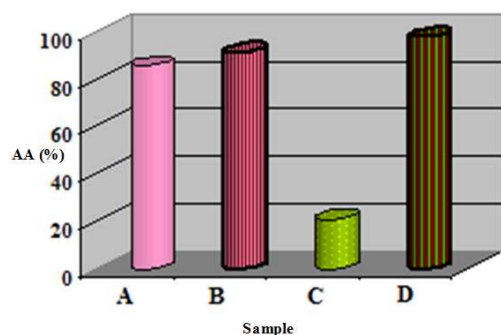


Fig. 9 Antioxidant activity values of the samples.

Antimicrobial activities of samples

The antimicrobial investigations carried out on both Gram-positive (*Staphylococcus aureus* ATCC 25923 and *Enterococcus faecalis* ATCC 29212) and Gram-negative (*Escherichia coli* ATCC 8738) bacteria revealed the biocidal activity of all the samples.

The cornelian aqueous extract exhibited antimicrobial activity against all three tested microorganisms offering diameters of inhibition zones ranging between 8.3 and 9.1 mm.

Chlorophyll *a* incorporated into artificial lipid bilayers (in a molar ratio of 1%) conferred to biomimetic membranes a slight antimicrobial activity against all three tested bacterial strains offering diameters of inhibition zones in the range 5.2 – 6.9 mm. The antimicrobial properties of this phytopigment are well recognized.^{46–48}

On the other hand, liposomes have the ability to fuse with the cell membrane inserting their content into the bacteria.

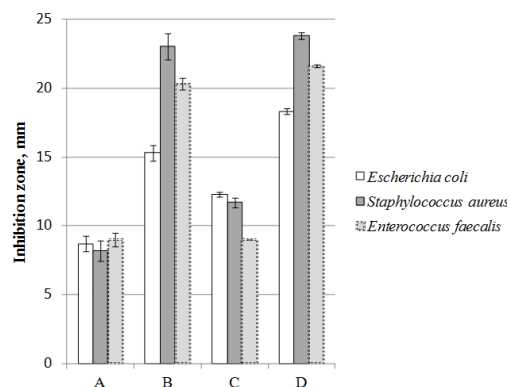


Fig. 10 Inhibition zone diameter for the microbial strains tested.

The cornelian silver nanoparticles (*Cornus*-AgNPs) synthesized using *Cornus mas* extract displayed strong biocidal properties offering inhibition zone of 15.1 mm, 23.1 mm and 20.4 mm against *Escherichia coli*, *Staphylococcus aureus* and *Enterococcus faecalis* respectively. Representative results of antibacterial activity of *Cornus*-AgNPs nanoparticles against *Staphylococcus aureus* are presented in Figure 10.

The maximum *in vitro* inhibition of tested microorganisms *Escherichia coli* ATCC 8738, *Staphylococcus aureus* ATCC 25923 and *Enterococcus faecalis* ATCC 29212 was recorded in silver –

based biohybrids (sample D) which offered inhibition zone of 18.3 mm, 23.8 mm and 21.6 mm respectively (Figure 10). It is well known that silver nanoparticles and carbon nanotubes possess antimicrobial properties.⁶² Small quantities of silver nanoparticles (AgNPs/MLVs = 1/30, v/v) and carbon nanotubes (0.05 mg/mL) were enough to achieve high antibacterial activity against all three microorganism strains. The high potency as biocides of these biohybrids could be explained also, by an efficient contact with the surface of bacteria provided by a combination of hydrophobic and electrostatic interactions resulting in perturbation of bacterial cell integrity and then cell membrane damage, the lipid component of these carbon-based hybrids playing a significant role in this process. Based on the results of the agar well diffusion method, the silver-based samples (B and D) exhibited highest values of antimicrobial activity, findings which could be explained not only by silver presence, but also by the nanometer nature of these samples (revealed by DLS measurements and AFM analysis) allowing stronger interactions with bacteria cell components. On the other hand, the small size and good dispersion state (non-aggregation) of a sample are favorable factors for bacteriostatic activity.^{16,63} Thus, according to DLS and zeta potential measurements, the silver-containing structures (see samples B and D) exhibited lower dimension and higher stability than liposomes alone.

The high antibacterial potential of the *C.mas*-AgNPs/Chla-DMPC-MLVs/CNTs hybrids allows their use as antimicrobial coating materials.

Conclusions

A novel simple and cost-effective *bottom-up* approach was developed to achieve antioxidant and antimicrobial cornelian biohybrids based on biomimetic membranes, phyto-nanosilver and single-walled carbon nanotubes. The originality of this scientific research work consists in the way of design, preparation and characterization of these new silver-based architectures starting from a natural raw material: *Cornus mas* L fruits.

„Green“ synthesis of AgNPs using the aqueous extract from *Cornus mas* L. cherries combines the benefits of these fruits with exciting properties of silver. The bioreducing power of cornelian extract was confirmed firstly by visual inspection (color changing) and supported by absorption spectra, DLS measurements and AFM images.

Chlorophyll *a* embedded in artificial lipid bilayers offered useful insights regarding the changes occurred in the biomimetic membranes at molecular level.

The absorption spectra showed that the addition of SWCNTs and phyto-nanosilver to a suspension of MLVs in physiological conditions (PB pH 7.4) resulted in spectral changes of Chla, rapidly sensing the formation of biohybrids.

The interfacing nanomaterials (such as carbon nanotubes, silver nanoparticles) with biomimetic systems (like liposomes) lead to improved hybrid materials. Small quantities of silver nanoparticles (AgNPs/MLVs = 1/30, v/v) and carbon nanotubes (0.05 mg/mL) were enough to assess high antimicrobial and antioxidant activities and also a good physical stability.

A good correlation between the visible absorption and fluorescence emission spectra, DLS measurements and AFM analysis was found.

Building cornelian silver-based architectures designed by a simple, low-cost *bottom-up* strategy opens the opportunity to use these

bioconstructs as coating materials to prevent oxidation and microorganism growth proliferation.

References

- 1 S. Iijima, *Nature*, 1991, **354**, 56–58.
- 2 P. C. Ma, N. A. Siddiqui, G. Marom and J. K. Kim, *Compos. Part A*, 2010, **41**, 1345–1367.
- 3 A. Jorio, R. Saito, G. Dresselhaus and M. S. Dresselhaus, in *Raman Spectroscopy in Graphene Related Systems*, WILEY-VCH Verlag GmbH & Co. KGaA, Weinheim, 2011, ch. 1, pp. 3–15.
- 4 Y. Zhang, Y. Bai and B. Yan, *Drug Discov. Today*, 2010, **15**(11–12), 428–435.
- 5 J. J. Castillo, T. Rindzevicius, L. V. Novoa, W. E. Svendsen, N. Rozlosnik, A. Boisen, P. Escobar, F. Martínez and J. Castillo-Léon, *J. Mater. Chem. B*, 2013, **1**, 1475–1481.
- 6 R. G. Mendes, A. Bachmatiuk, B. Büchner, G. Cuniberti and M. H. Rummeli, *J. Mater. Chem. B*, 2012, **1**, 401–429, DOI: 10.1039/c2tb00085g.
- 7 Z. Liu, S. Tabakman, K. Welsher and H. Dai, *Nano Res.*, 2009, **2**, 85–120.
- 8 P. Prema, in *Progress in Molecular and Environmental Bioengineering - From Analysis and Modeling to Technology Applications*, ed. A. Carpi, Publisher: InTech, 2011, ch.6, pp.151–166.
- 9 C. Ungureanu, D. Ionita, N. Badea and I. Demetrescu, *Dig. J. Nanomater. Bios.*, 2011, **6**(3), 1273–1279.
- 10 Y. Wang, B. B. Newell and J. Irudayaraj, *J. Biomed. Nanotechnol.*, 2012, **8**(5), 751–759.
- 11 G. Yang, Q. Lin, C. Wang, J. Li, J. Wang, J. Zhou, Y. Wang and C. Wang, *J. Nanosci. Nanotechnol.*, 2012, **12**(5), 3766–3774.
- 12 C.-H. Tu and S.-S. Lo, *J. Nanosci. Nanotechnol.* 2011, **11**(12), 10575–10578.
- 13 A. Hekmat, A. A. Saboury and A. Divsalar, *J. Biomed. Nanotechnol.*, 2012, **8**, 968–982.
- 14 S. Taheri, G. Baier, P. Majewski, M. Barton, R. Förch, K. Landfester and K. Vasilev, *J. Mater. Chem. B*, 2014, **1**, DOI: 10.1039/C3TB21690J.
- 15 C. Damm, H. Münstedt and A. Rösch, *Mater. Chem. Phys.*, 2008, **108**(1), 61–66.
- 16 T.-Yen Chi, H.-Y. Yeh, J.-J. Lin, U.-S. Jeng and S.-H. Hsu, *J. Mater. Chem. B*, 2013, **1**, 2178–2189.
- 17 Q. Shi, N. Vitshuli, J. Nowak, J. Noar, J. M. Caldwell, F. Breidt, M. Bourham, M. McCord and X. Zhang, *J. Mater. Chem.*, 2011, **21**, 10330–10335.
- 18 M. E. Barbinta-Patrascu, I. R. Bunghez, S. M. Iordache, N. Badea, R. C. Fierascu and R. M. Ion, *J. Nanosci. Nanotechnol.*, 2013, **13**, 2051–2060.
- 19 C. Ramteke, T. Chakrabarti, B. K. Sarangi and R.-A. Pandey, *Journal of Chemistry*, 2013, **1**–7, <http://dx.doi.org/10.1155/2013/278925>.
- 20 R. Bunghez, M. E. Barbinta Patrascu, N. Badea, S. M. Doncea, A. Popescu and R. M. Ion, *J. Optoelectron. Adv. M.*, 2012, **14**(11–12), 1016 – 1022.
- 21 V. K. Sharma, R. A. Yngard and Y. Lin, *Adv. Colloid Interface Sci.*, 2009, **145**, 83–96.
- 22 R. W. Rajesh, L. R. Jaya, K. S. Niranjana, M. D. Vijay and K. B. Sahebrao, *Curr. Nanosci.*, 2009, **5**, 117–122.
- 23 S. Mashaghi, T. Jadidi, G. Koenderink and A. Mashaghi, *Int. J. Mol. Sci.*, 2013, **14**, 4242–4282.
- 24 I. Lacatusu, N. Badea, O. Oprea, D. Bojin and A. Meghea, *J. Nanopart. Res.*, 2012, **14**, 902–917.
- 25 I. Lacatusu, N. Badea, A. Murariu and A. Meghea, *Nanoscale Res. Lett.*, 2011, **6**, 73 – 82.
- 26 S. Aryal, C.-M. J. Hu, V. Fu and L. Zhang, *J. Mater. Chem.*, 2012, **22**, 994–999.
- 27 T. N. Duc, R. El Zein, J.-M. Raimundo, H. Dallaporta and A. M. Charrier, *J. Mater. Chem. B*, 2013, **1**, 443–446.
- 28 M. E. Barbinta Patrascu, A. Cojocariu, L. Tugulea, N. Badea, I. Lacatusu and A. Meghea, *J. Optoelectron. Adv. M.*, 2011, **13**(9), 1165–1170.
- 29 Y. Huang, P. V. Palkar, L. J. Li, H. Zhang and P. Chen, *Biosens. Bioelectron.*, 2010, **25**, 1834–1837.
- 30 J. C. Debouzy, D. Crouzier and E. Flahaut, *Env. Toxicol. Pharmacology*, 2010, **30**(2), 147–152.
- 31 H. Xing, L. Tang, X. Yang, K. Hwang, W. Wang, Q. Yin, N. Y. Wong, L. W. Dobrucki, N. Yasui, J. A. Katzenellenbogen, W. G. Helferich, J. Cheng and Y. Lu, *J. Mater. Chem. B*, 2013, **1**, 5288–5297.
- 32 A. Hashempour, R. F. Ghazvini, D. Bakhshi, M. Ghasemnezhad, M. Sharafati and H. Ahmadian, *Horticulture, Environment and Biotechnology*, 2010, **51**, 83–88.
- 33 N. Ersoy, Y. Bagci and V. Gok, *Sci. Res. Essays*, 2011, **6**, 98–102.
- 34 I. Gulcin, S. Beydemir, I. G. Sat and O. I. Kufrevioglu, *Acta Aliment. Hung.*, 2005, **34**, 193–202.
- 35 B. J. West, S. Deng, C. J. Jensen, A. K. Palu and L. F. Berrio, *Int. J. Food Sci. Tech.*, 2012, **47**, 1392–1397.
- 36 A. M. Pawlowska, F. Camangi and A. Braca, *Food Chem.*, 2010, **119**, 1257–1261.
- 37 S. M. Milenkovic, M. E. Barbinta-Patrascu, G. Baranga, D. Z. Markovic and L. Tugulea, *Gen. Physiol. Biophys.*, 2013, **32**(4), 559–567.
- 38 M. E. Barbinta Patrascu, L. Tugulea, I. Lacatusu and A. Meghea, *Mol. Cryst. Liq. Cryst.*, 2010, **522**, 148–158.
- 39 T. Stefanescu, C. Manole, C. Parvu, M. E. Barbinta Patrascu and L. Tugulea, *Optoelectron. Adv. Mat.- Rapid Commun.*, 2010, **4**(1), 33–38.
- 40 M. E. Barbinta Patrascu, L. Tugulea and A. Meghea, *Rev. Chim.*, 2009, **60**(4), 337–341.
- 41 M. E. Barbinta Patrascu, L. Tugulea, A. Meghea and A. Popescu, *Optoelectron. Adv. Mat.- Rapid Commun.*, 2008, **2**(2), 113–116.
- 42 M. E. Barbinta Patrascu, N. Badea, L. Tugulea, M. Giurginca and A. Meghea, *Rev. Chim.*, 2008, **59**(8), 834–837.
- 43 D. Garg, A. Muley, N. Khare and T. Marar, *Research Journal of Pharmaceutical, Biological and Chemical Sciences*, 2012, **3**(3), 845–854.
- 44 P. L. Dentuto, L. Catucci, P. Cosma, P. Fini, A. Agostiano, S. Hackbarth, F. Rancan and B. Roeder, *Bioelectrochemistry*, 2007, **70**, 39–43.

- 45 U. M. Lanfer-Marquez, R. M. C. Barros and P. Sinnecker, *Food Res. Int.*, 2005, **38**, 885-891.
- 46 O. Habbal, S. S. Hasson, A. H. El-Hag, Z. Al-Mahrooqi, N. Al-Hashmi, Z. Al-Bimani, M. S. Al-Balushi and A. A. Al-Jabri, *Asian Pacific Journal of Tropical Biomedicine*, 2011, **1**(3), 173-176.
- 47 P. Jayavanth, K. Kaur and A. H. Junainah, *J. Nat. Prod.*, 2011, **4**, 94-99.
- 48 L. E. Maekawa, R. Lamping, S. Marcacci, M. Y. Maekawa, M. R. G. Nassri and C. Y. Koga-Ito, *RSBO*, 2007, **4**(2), 36-40.
- 49 R. R. C. New, *Liposomes: A Practical Approach*, IRL Press, Oxford University, 1990.
- 50 H. H. Strain and W. A. Svec, in *The chlorophylls*, ed. L. P. Vernon and G. R. Seely, New York: Academic Press, 1966, ch. 2, pp. 21-66.
- 51 R. Augustine and K. Rajarathinam, *Int. J. Nano Dim.*, 2011, **2**(3), 205-212.
- 52 T. Elavazhagan and K. D. Arunachalam, *Int. J. Nanomed.*, 2011, **6**, 1265-1278.
- 53 J. Kasthuri, K. Kathiravan and N. Rajendiran, *J. Nanopart Res.*, 2009, **11**, 1075-1085.
- 54 K. B. Narayanan and N. Sakthivel, *Mater. Lett.*, 2008, **62**, 4588-4590.
- 55 A. J. Kora, S. R. Beedu and A. Jayaraman, *Org. Med. Chem. Lett.*, 2012, **2**(1), 17, doi:10.1186/2191-2858-2-17.
- 56 L. Tugulea and S. Pascanu, *Rom. J. Biophys.*, 1996, **6**, 1-10.
- 57 S. A. Wissing and R. H. Müller, *J. Control. Release*, 2002, **81**, 225-233.
- 58 G. Merényi, J. Lind and T. E. Eriksen, *J. Biolumin. Chemilumin.*, 1990, **5**, 53-56.
- 59 J. Lind, G. Merényi and T. E. Eriksen, *J. Am. Chem. Soc.*, 1983, **105**, 7655-7661.
- 60 D. F. Roswell and E. H. White, in *Meth. Enzymol.* 57, ed. S. Fleischer and B. Fleischer, 1978, ch 36, pp. 409-423.
- 61 C. Nichita and I. Stamatina, *Dig. J. Nanomater. Bios.*, 2013, **8**(1), 445-455.
- 62 A. J. Huh and Y. J. Kwon, *J. Control. Release*, 2011, **156**, 128-145.
- 63 S. H. Hsu, H. J. Tseng and Y. C. Lin, *Biomaterials*, 2010, **31**, 6796-6808.